**Supplementary material:**

## A1. Calculation of $\Delta_{47}$ values in the absolute reference frame

$\Delta_{47}$ values in the main text are reported using the original clumped isotope reference frame, as was used in the $\Delta_{47}$-T calibration of Ghosh et al. (2006) (noted as 'lab frame'). The data is given in Table S1 also using a new absolute reference frame (Dennis et al., 2011). The absolute reference frame is based on the measurement of $CO_2$ equilibrated with $H_2O$ at different temperatures having defined absolute $\Delta_{47}$ values that are based on *ab-initio* calculations (Wang et al., 2004).

The conversion of $\Delta_{47}$ values from the laboratory frame to the absolute frame uses the long-term average of laboratory standards (Carrara Marble, $CO_2$ gas equilibrated with water at 25 °C, $CO_2$-gas standard). The heated gas value at 1000 °C is considered as an additional calibration point in the calculation.

## A2. Evaluation of the speleothem fluid inclusion noble gas data

Noble gases and water were liberated from the stalagmite samples in a stepwise procedure. This stepwise extraction leads sometimes to differences between subsequent steps due to preferential opening of inclusions of a certain size (Marx and Aeschbach-Hertig, 2012). In the first step mostly large air-filled inclusions at grain boundaries are opened, whereas in later steps the gases increasingly originate from smaller, intra-crystalline water-filled inclusions (Scheidegger et al., 2011). In order to avoid aliasing we take the combined noble gas concentration of all steps as the most reliable value. In cases where the combined signal could not be used (e.g. due to a too high air/water volume ratio, Kluge et al., 2008) we evaluated the single steps by the inverse method of Aeschbach-Hertig et al. (1999) and selected the extraction step with the best fit, namely the step with the lowest $\chi^2$. We use $\chi^2$, the sum of the error-weighted squared deviations of the measured noble gas concentration from the modeled concentrations, to judge the quality of the fit. The expectation value for $\chi^2$ is 2

(four measured concentrations and two free parameters) and with a probability of 0.99 to be smaller than 9.2. $\chi^2$ values above 9.2 indicate a bad fit and are therefore generally rejected. Noble gas concentrations, $\chi^2$, and the fitted temperature of the relevant extraction steps are summarized in Table S2.

NGTs from stalagmites BU1 and BU-UWE show consistently too low temperatures relative to the regional 1961-1990 mean. This deviation is likely due to analytical artefacts and unrelated to environmental influences. During studies that aimed at improving the technique it was realized that the combined analysis of all heavy noble gases in one measurement step leads to an overestimation of the Kr and Xe fraction (Marx et al., 2010; Wieser, 2011). Overestimated concentrations of heavy noble gases lead to lower apparent temperatures and are one possible explanation for our results. A slight underestimation of water amounts during the crushing steps (due to water adsorption on freshly crushed calcite) similarly causes too high apparent noble gas concentrations and too low NGTs. Tests showed that temperatures during the final heating step were high enough to completely release potentially adsorbed water. By combining water and gas amounts of all steps or all steps without the first one, which is dominated by gases from air-filled inclusions, we exclude (or at least minimize) a possible influence of water adsorption on the determined NGT, obtaining more reliable NGT values. A constant offset correction, i.e., independent of the speleothem growth period, is justified because the deviations were consistently caused by analytical artefacts (such as by the influence of Ar on the Kr and Xe signal) and not by environmental influences. An indication for a consistent offset due to an analytical artefact are the reproducible early Holocene NGTs (Kluge et al., 2008) and the consistency of Holocene NGTs from the same time interval (BU1-B and BU1-C; BU1-D,E,F,G).

## A3. Value of the co-variation slope determined from Holocene stalagmites

The application of the $\Delta_{47}$- $\delta^{18}O$ co-variation method for paleoclimate reconstruction is based on the assumption of a constant co-variation slope over time. The precise investigation of this assumption is difficult as it requires high-precision temperature and water $\delta^{18}O$ data from the sample location for the past. The offsets of the Holocene parts of stalagmites BU1 and BU4 shown in Fig. 2 were calculated for illustration purposes assuming a constant drip-water $\delta^{18}O$ value of -7.9 ‰ and a constant temperature of 9.5°C (8.5°C for sample BU4-9). This assumption was made for simplicity and is only applied for offset calculation for BU1 and BU4 samples and not for the actual drip-water reconstruction. For drip-water reconstruction the water $\delta^{18}O$ value is the unknown, whereas the temperature is taken from independent paleotemperature studies.

The actual climatic parameters likely deviated slightly from the assumed constant temperature and drip water $\delta^{18}O$ value used for the illustrative offset calculation in Fig. 2 (as seen in variations in the reconstructed water $\delta^{18}O$ values of this study). Also, regional temperature variations of up to 2°C are likely. Global or hemispheric reconstructions (as e.g., by Mann et al., 2008) show a smoothed picture that suppresses climatic excursions at the regional scale. Such deviations may shift the $\delta^{18}O$ offset by 0.5 ‰ for 2°C. This value is substantial compared to the extent of the kinetic isotope fractionation in speleothems (~ 1 ‰). Thus, the deviation of the $\Delta_{47}$-$\delta^{18}O$ co-variation slope of BU1 and BU4 from the modern values and each other is likely due to slight deviations of the used reference temperature from actual values (and to a smaller extent to the drip-water $\delta^{18}O$ uncertainty). Furthermore, displaying the $\Delta_{47}$ and $\delta^{18}O$ offsets for both stalagmites separately (Panel A and B in Fig. S1) shows that most samples agree with the modern $\Delta_{47}$-$\delta^{18}O$ co-variation slope within uncertainty (the dotted line in Fig. S1 corresponds to the ± 0.3 ‰ uncertainty of the modern drip-water measurements). Samples that deviate from the modern slope likely reflect climatic

conditions that deviate from the assumed temperature and drip-water $\delta^{18}O$ value (e.g., during the Holocene Climatic Optimum).

**Additional references**

Marx, T., Kluge, T., Mangini, A., and Aeschbach-Hertig, W.: Advances in noble gas paleothermometry on speleothems, Geophys. Res. Abstracts, 12, EGU2010-13393, 2010.

Marx, T. and Aeschbach-Hertig, W.: Challenges on the way to noble gas temperatures on speleothems, Geophys. Res. Abstracts, 14, EGU2012-9621, 2012.

Wieser, M.: Imprints of climatic and environmental change in a regional aquifer system in an arid part of India using noble gases and other environmental tracers, PhD thesis, Universität Heidelberg, Heidelberg, Germany, 2011.

**Table S1**:

$\Delta_{47}$ values in the original reference frame (lab frame) and the newly defined absolute reference frame (Dennis et al., 2011).

| Sample | $\Delta_{47}$ lab frame (‰) | $\Delta_{47, abs}$ (‰) |
|---|---|---|
| Modern set | | |
| DC-1 | 0.648±0.005 | 0.708±0.006 |
| DC-2 | 0.657±0.004 | 0.718±0.005 |
| | | |
| HC-1 | 0.674±0.004 | 0.736±0.004 |
| HC-2 | 0.687±0.004 | 0.749±0.005 |
| HC-3 | 0.671±0.002 | 0.732±0.002 |
| HC-4 | 0.689±0.001 | 0.751±0.002 |
| | | |
| B7-B01 | 0.668±0.006 | 0.729±0.007 |
| | | |
| U I-4 | 0.668±0.020 | 0.729±0.021 |
| U I-16 | 0.665±0.008 | 0.726±0.009 |
| U IV-15 | 0.638±0.020 | 0.697±0.021 |
| U VII-5 | 0.670±0.020 | 0.731±0.021 |
| U VII-8 | 0.653±0.020 | 0.713±0.021 |
| U VII-14 | 0.675±0.020 | 0.737±0.021 |
| U VII-15 | 0.658±0.003 | 0.718±0.003 |
| | | |
| Stalagmite BU1 | | |
| 1 | 0.659±0.007 | 0.720±0.007 |
| 2 | 0.673±0.002 | 0.734±0.002 |
| 3 | 0.670±0.009 | 0.731±0.010 |
| 4 | 0.685±0.002 | 0.748±0.002 |
| 5 | 0.676±0.005 | 0.738±0.005 |
| 6 | 0.679±0.003 | 0.740±0.003 |

| | | |
|---|---|---|
| 7 | 0.678±0.008 | 0.740±0.009 |
| 8 | 0.681±0.007 | 0.743±0.007 |
| 9 | 0.693±0.002 | 0.755±0.002 |
| 10 | 0.671±0.007 | 0.732±0.008 |
| | | |
| Stalagmite BU4 | | |
| 1 | 0.668±0.007 | 0.729±0.007 |
| 2 | 0.677±0.003 | 0.739±0.003 |
| 3 | 0.671±0.003 | 0.732±0.003 |
| 4 | 0.669±0.007 | 0.731±0.007 |
| 5 | 0.677±0.006 | 0.739±0.006 |
| 6 | 0.667±0.004 | 0.728±0.004 |
| 7 | 0.676±0.004 | 0.738±0.004 |
| 8 | 0.692±0.005 | 0.754±0.005 |
| 9 | 0.705±0.005 | 0.768±0.005 |
| | | |
| Stalagmite BU2 | | |
| 1 | 0.674±0.007 | 0.735±0.007 |
| 2 | 0.669±0.005 | 0.730±0.005 |
| 3 | 0.702±0.007 | 0.765±0.007 |
| 4 | 0.696±0.007 | 0.759±0.008 |
| | | |
| Stalagmite BU-UWE | | |
| 1 | 0.667±0.005 | 0.728±0.005 |
| 2 | 0.663±0.005 | 0.724±0.006 |
| 3 | 0.663±0.004 | 0.723±0.004 |
| 4 | 0.692±0.005 | 0.754±0.005 |
| 5 | 0.662±0.008 | 0.722±0.008 |
| 6 | 0.668±0.003 | 0.729±0.003 |
| 7 | 0.676±0.011 | 0.738±0.011 |

**Table S2**: Noble gas concentrations (in ccSTP per g water), $\chi^2$, extraction steps used for inverse modeling, and NGTs of stalagmite BU1. Data of BU-UWE (Kluge et al., 2008) are given for completeness. The extraction typically consists of 2-3 crushing steps and a final heating step. The first extraction step was normally discarded due to a high air contribution.

| Sample | Ne ($10^{-7}$cc/g) | Ar ($10^{-4}$cc/g) | Kr ($10^{-7}$cc/g) | Xe ($10^{-8}$cc/g) | $\chi^2$ (-) | Used extraction steps | NGT (°C) |
|---|---|---|---|---|---|---|---|
| BU 1-A | 17.1±0.3 | 11.3±0.2 | 1.87±0.04 | 2.17±0.04 | 4.9 | All[a] | 7.1±0.8 |
| BU1-B | 8.3±0.3 | 7.6±0.2 | 1.40±0.05 | 1.68±0.07 | 3.0 | thermal extraction step | 7.1±1.1 |
| BU1-C | 23.8±0.5 | 14.9±0.3 | 2.28±0.05 | 2.51±0.08 | 1.7 | all except first | 7.3±1.4 |
| BU1-D I | 76.6±2.5 | 40.5±1.4 | 5.5±0.2 | 4.9±0.2 | 0.9 | all except first | 9.8±5.6 |
| BU1-D II | 20.7±0.5 | 12.9±0.2 | 2.04±0.04 | 2.21±0.06 | 2.8 | all except first | 9.5±1.3 |
| BU1-E | 36.7±0.7 | 21.9±0.4 | 3.16±0.07 | 3.04±0.08 | 0.3 | all | 7.9±1.6 |
| BU1-F | 4.3±0.3 | 5.2±0.2 | 1.08±0.04 | 1.43±0.06 | 0.7 | all except first | 9.0±1.1 |
| BU1-G I | 5.6±0.6 | 5.6±0.5 | 1.11±0.09 | 1.5±0.1 | 0.1 | thermal extraction step | 10.0±2.3 |
| BU1-G II | - | 7.57±0.09 | 1.44±0.03 | 1.70±0.04 | 4.6 | all except first | 7.5±0.9 |
| BU-UWE | | | | | | | |
| Early Holocene | | | | | 1.1-9.3 | see Kluge et al. (2008) | 1.7-3.6 |

[a] only one extraction step (crushing)

**Figures:**

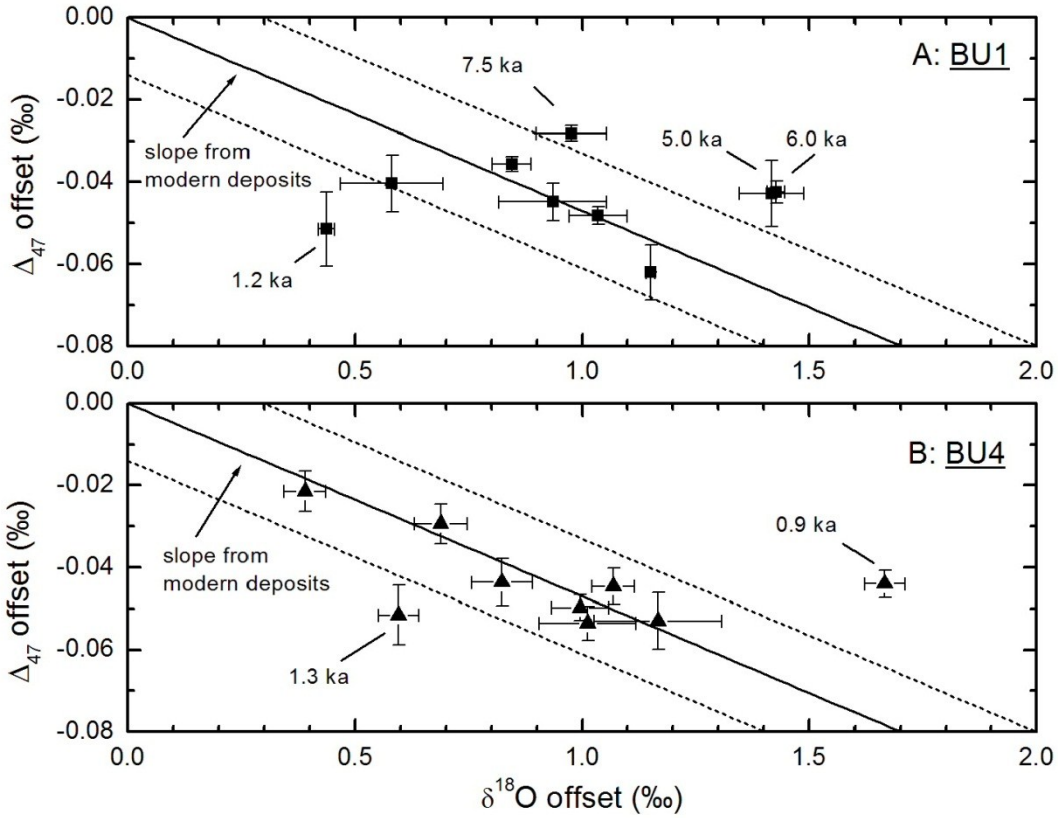


**Figure S1:**

$\Delta_{47}$ and $\delta^{18}O$ offsets of stalagmites BU1 (A) and BU4 (B). The offsets are calculated assuming a constant drip-water $\delta^{18}Ow$ value of -7.9‰ and a constant temperature of 9.5°C (8.5°C for BU4-9). Samples that deviate from the modern $\Delta_{47}$-$\delta^{18}O$ co-variation slope are marked with ages and likely reflect a deviation from the constant temperature or constant $\delta^{18}Ow$ assumption.

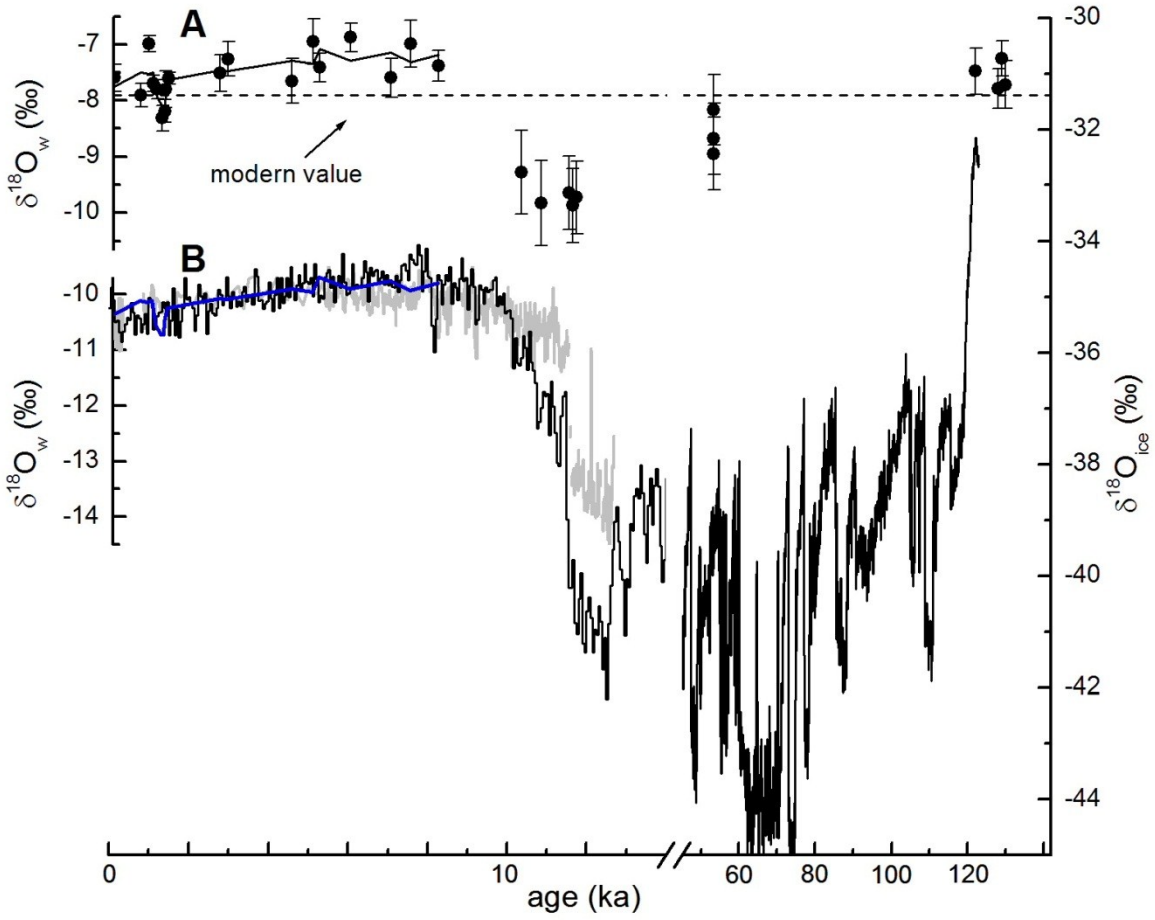


**Figure S2:**

Reconstructed drip-water $\delta^{18}O$ values (A), rainfall $\delta^{18}O$ values inferred from Lake Ammersee ostracods (B, light grey; von Grafenstein et al., 1999) and water isotopes evolution in Greenland (B, black; NGRIP members 2004). All data sets are shown on the same scale. The Holocene trend of the drip-water reconstruction is shown for comparison in panel B as a blue line.